A G_s-Selective Analog of the Receptor-Mimetic Peptide Mastoparan Binds to $G_s\alpha$ in a Kinked Helical Conformation†

Muppalla Sukumar,*,‡ Elliott M. Ross,§ and Tsutomu Higashijima||

Department of Chemistry, University of Massachusetts at Amherst, Amherst, Massachusetts 01003, and Department of Pharmacology, University of Texas Southwestern Medical Center, Dallas, Texas 75235-9041

Received September 18, 1996; Revised Manuscript Received January 7, 1997⊗

ABSTRACT: Mastoparan, a 14-residue peptide, stimulates GDP/GTP exchange on G proteins in a manner strikingly analogous to that of agonist-bound receptors. Presumably, the peptide structurally mimics a receptor's G protein-binding domain. We previously reported that mastoparan-X binds to α-subunits of G_i and G_o in a predominantly α-helical conformation [Sukumar, M., & Higashijima, T. (1992) *J. Biol. Chem. 267*, 21421−21424]. We have now developed an analogous peptide, INWKGIASM-α-aminoisobutyryl (Aib)-RQVL-NH_2 (MP-S), which is a selective activator of G_s. We report the conformation of MP-S when it is bound to $G_s\alpha$, determined from distance geometry calculations based on transferred nuclear Overhauser effects (TRNOEs). The G_s-bound conformation of MP-S is an α-helix that is kinked at residue 9. The conformations of MP-S when bound to $G_i\alpha$ or $G_o\alpha$ are similar to the $G_s\alpha$-bound conformation. In contrast, the lipid-bound conformation of MP-S is a straight helix. On the basis of the G_s-bound conformation of MP-S, directions for the design of G_s-selective peptidergic mimics of receptors are suggested.

Mastoparans, a family of tetradecapeptides originally isolated from wasp venom, catalyze GDP/GTP exchange on G proteins through a mechanism remarkably similar to that of G protein-coupled receptors (Higashijima *et al*., 1988). Because G proteins are activated by bound GTP, mastoparans thus function as receptor surrogates to initiate signaling. The functional similarity between mastoparan and the receptors, and the apparent competition between them for binding to G protein α-subunits (Higashijima *et al*., 1988, 1990), suggest that mastoparan binds to G proteins at the receptor-binding site. Furthermore, it is likely that mastoparan, in its G protein-bound conformation, mimics the G protein-binding domains on receptors that have been tentatively assigned to the C- and N-terminal segments of the third intracellular loop (O'Dowd *et al*., 1989; Ross, 1989; Strader *et al*., 1989). These regions have positively charged residues and can be modeled as amphipathic α-helices.

We recently determined the G protein-bound conformation of mastoparan-X (MP-X)[1] using TRNOE methods (Sukumar & Higashijima, 1992). TRNOESY has been widely used to determine conformations of small ligands bound to large proteins or molecular aggregates like liposomes (Clore & Gronenborn, 1982, 1983; Campbell & Sykes, 1991, 1993; Sukumar & Higashijima, 1992). TRNOESY works optimally when the bound ligand is in fairly rapid equilibrium with an excess of free ligand. The EC_{50}s of mastoparans for G protein activation are ∼10 μM, and substantial TRNOEs are expected for affinities in this range (Sukumar & Higashijima, 1992). The TRNOE method relies on transfer of cross-relaxation between two nuclei in the bound state to the free ligand resonances via chemical exchange of free and bound ligand and is observed as a negative NOE between free ligand resonances. Because the cross-relaxation rate is a sensitive function of interproton distance, the TRNOE technique serves as a means of identifying spatially close (<5 Å) protons in the bound form (Wuthrich *et al*., 1983; Wuthrich, 1986). TRNOE data provide an approximate set of interproton distance constraints, which are then used to arrive at the conformation of the bound form.

TRNOESY data indicated that MP-X adopts a predominantly α-helical conformation when bound to G proteins (Sukumar & Higashijima, 1992). The G protein-bound conformation of MP-X is very similar to its membrane-bound conformation, reported by us previously (Wakamatsu *et al*., 1992), but differs from the largely unordered structure that MP-X adopts in aqueous buffers (Higashijima *et al*., 1983, 1984; Wakamatsu *et al*., 1983). The α-helical folding of MP-X places the polar Lys residues on one face of the helix and clusters the hydrophobic residues on the opposite face, making the overall structure amphipathic. The similarity of the G protein-bound and membrane-bound conformations of MP-X is consistent with the fact that activation of G proteins by mastoparans is much more pronounced when G proteins

† These studies were supported by United States Public Health Service Grants R01GM40676 to T.H. and R37GM30355 to E.M.R. and R. A. Welch Foundation Grant I-0982 to E.M.R.

* Address correspondence to Dr. Muppalla Sukumar, Department of Chemistry, University of Massachusetts, Amherst, MA 01003. Phone: (413) 545-0625. Fax: (413) 545-0011. E-mail: sukumar@chemistry.umass.edu.

‡ University of Massachusetts at Amherst.

§ University of Texas Southwestern Medical Center.

|| Deceased.

⊗ Abstract published in *Advance ACS Abstracts,* March 15, 1997.

[1] Abbreviations: Aib, α-aminoisobutyric acid; DG, distance geometry; DPPC-d_{80}, perdeuterated dipalmitoylphosphatidylcholine; FID, free induction decay; r$G_s\alpha$, recombinant $G_s\alpha$ produced in *Escherichia coli*; GTPγS, guanosine 5′-3-*O*-(thio)triphosphate; MP, mastoparan (INLKALAALAKKIL); Mas7, Ala[12],Leu[13]-mastoparan; MP-S, Trp[3],Gly[5],-Ile[6],Ser[8],Met[9],Aib[10],Arg[11],Gln[12],Val[13]-mastoparan; MP-X (mastoparan-X, Trp[3],Gly[5],Ile[6],Met[9],Leu[13]-mastoparan); NOE, nuclear Overhauser effect; NOESY, nuclear Overhauser effect spectroscopy; TMSP, 3-(trimethylsilyl)propionic acid; TOCSY, total correlation spectroscopy; TRNOE, transferred nuclear Overhauser effect; TRNOESY, transferred nuclear Overhauser effect spectroscopy.

S0006-2960(96)02356-2 CCC: $14.00

are reconstituted in lipid vesicles than when their activity is measured in detergent solution (Higashijima *et al*., 1988). Structure−activity relationships of mastoparan analogs show that both the ability to form an amphipathic helix and the presence of positively charged residues at N- and C-terminal ends of the helix are crucial for regulatory activity (Higashijima *et al*., 1990). Thus, the polar face of the amphipathic MP-X molecule is probably involved in the binding interaction.

Mutually selective interaction between receptors and G proteins determines the signaling pathways that are initiated by an individual receptor, and mastoparans display less marked but still significant selectivity among G proteins. Mastoparan is modestly selective for G_is, G_z, and G_o, closely related G proteins that mediate inhibition of adenylylcyclase and the regulation of diverse ion channels. Mastoparan is much less effective in stimulating G_s, which activates adenylylcyclase, or G_q, which stimulates phospholipase C-β (Higashijima *et al*., 1988; Casey & Gilman, 1988; Taylor *et al*., 1991). Regulatory peptides with marked specificity for individual G proteins would be useful molecular tools in studies aimed at delineating the involvement of a particular G protein in specific biochemical pathways (Eker *et al*., 1994; Colombo *et al*., 1994; Murga *et al*., 1996) and, potentially, as prototypes for development of G protein-directed drugs. As part of a program to develop G protein-selective peptides, we used TRNOESY to examine the conformation of mastoparans when bound to various G proteins. We initially examined the conformation of MP-X bound to $G_i\alpha$ and $G_o\alpha$ (Sukumar & Higashijima, 1992). Although the observed TRNOEs were consistent with an α-helical conformation for the G protein-bound MP-X, the degenerate nature of the MP-X sequence and the effects of conformational averaging resulted in extensive overlap of NMR signals corresponding to the C-terminal half of the molecule which made it difficult to ascertain the presence or absence of several key interresidue TRNOEs. In an attempt to further refine the G protein-bound conformation of mastoparans, we developed mastoparan analogs that have less degenerate sequences in the C-terminal half. In developing these analogs, we have taken into consideration the structural requirements for activity, like the positioning of positive charges, net hydrophobicity, and overall amphipathicity (Higashijima *et al*., 1990).

One of the recently developed analogs of mastoparan, MP-S (INWKGIASM-Aib-RQVL-NH_2), not only gave a good dispersion of ^{1}H-NMR signals, allowing unambiguous assignment of most of the TRNOEs, but also had the interesting property of activating G_s more markedly than G_o and G_i. This is in contrast to all other mastoparan analogs that we have examined, which activate G_i and G_o better than they activate G_s (Higashijima *et al*., 1988). This observation supports the idea that regulatory peptides specific for individual G proteins, which are otherwise highly homologous, can in fact be found within the simple framework of a relatively small molecule. In the development of the MP-S analog, the unusual amino acid Aib was introduced at position 10 with the expectation that, due to its unique ability to stabilize α-helical conformations (Karle & Balaram, 1990), the H^α chemical shifts of residues in its neighborhood will be shifted from their random coil values.

In this report, we describe the conformation assumed by MP-S when bound to $G_s\alpha$ determined by TRNOESY and distance geometry calculations and show that its G protein-bound conformation is a kinked helix, distinct from the membrane-bound conformation, which is a straight helix. On the basis of the G_s-bound conformation of MP-S, we suggest useful directions for the design of G_s-selective peptidergic mimics of receptors.

EXPERIMENTAL PROCEDURES

Peptide Synthesis. Peptides were synthesized by standard solid phase procedures. The crude peptide was purified to apparent homogeneity by reverse phase HPLC on a Vydac C4 column, and the purity was confirmed by amino acid analysis and NMR spectroscopy.

Protein Purification and Assays. Recombinant $G_s\alpha$, $G_o\alpha$, and $G_i\alpha$ expressed in *Escherichia coli* were purified according to reported procedures (Itoh & Gilman, 1991; Linder & Gilman, 1991), with minor modifications. Protein fractions obtained after Mono Q chromatography were >90% pure by SDS-PAGE and were used for NMR experiments without further purification. Preparation of protein samples for NMR spectroscopy (Sukumar & Higashijima, 1992) and measurement of [^{35}S]GTPγS binding and MP-S-promoted GTPase activity (Northup *et al*., 1982; Higashijima *et al*., 1987, 1988) were performed as described previously. G$\beta\gamma$ was purified from bovine brain and reconstituted with Gα-subunits as described previously (Higashijima *et al*., 1988).

Preparation of Small Unilamellar Vesicles. Perdeuterated DPPC was a kind gift from K. Wakamatsu (Gunma University, Kiryu, Japan). Small unilamellar vesicles were prepared as follows. A thin film of DPPC-d_{80} obtained by evaporating a chloroform solution of the lipid was suspended in NMR sample buffer (5 mM KP_i, 25 mM NaCl) and sonicated using a probe type sonicator at 20 W for a total of 30 min at 60 °C. Vesicles obtained by this procedure are expected to have a diameter of 200−300 Å (Wakamatsu *et al*., 1992).

NMR Spectroscopy. All the NMR experiments were carried out on a Varian VXR500 NMR spectrometer at 20 °C and pH 6.0 in phosphate buffer (5 mM) in the presence of 25 mM NaCl, in a total sample volume of 0.7 mL. Fifty microliters of D_2O was included to serve as an internal field-frequency-lock. TRNOESY spectra were recorded at a mixing time of 100 ms. Previous experiments with MP-X (Sukumar & Higashijima, 1992) showed that the best signal-to-noise ratio in the amide region was obtained at pH 6.0 and that the magnitudes of TRNOEs were linear up to a mixing time of 100 ms. MP-X-stimulated GTPase activities were almost identical at pH 6.0 and 8.0. GTPγS binding activity was measured after every NMR experiment, and specific GTPγS binding activity after the NMR experiment was always 80−100% of that of the initial protein sample, suggesting that G protein α-subunits are fairly stable under these conditions.

TOCSY (Davis & Bax, 1985) and NOESY (Jeener *et al*., 1979; Kumar *et al*., 1981; Macura *et al*., 1981) spectra were obtained using standard pulse schemes. A total of 256 FIDs were acquired using a spectral width of 6000 Hz, with 2k data points and 32 or 128 scans for each FID. A mixing time of 75 ms was used for the TOCSY experiment. Data were processed using the program FTNMR (Hare Research Inc., Seattle, WA). One-dimensional spectra were measured with 32k data points and a spectral width of 6000 Hz. Chemical shifts were measured relative to an internal standard, TMSP.

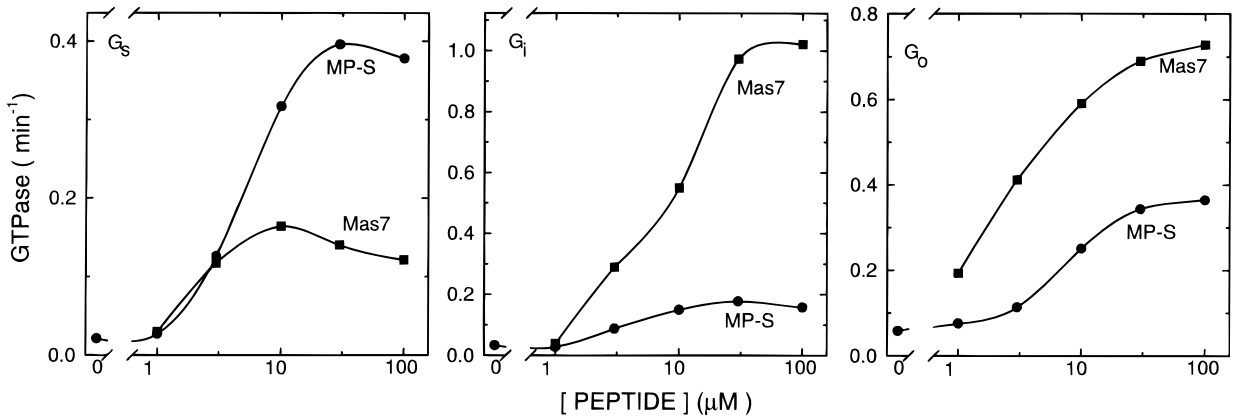

FIGURE 1: G protein selectivity of MP-S. The steady-state GTPase activities of G_s, G_i, and G_o were assayed in the presence of either MP-S or Mas7 (Ala[12], Leu[13]-mastoparan) shown on the abscissa under conditions where GTP/GDP exchange is rate-limiting (Higashijima *et al*., 1990). Data are calculated as molar turnover numbers by dividing specific GTPase activity by the molar concentration of Gα subunit determined by GTPγS binding. Trimeric G proteins were prepared by mixing the appropriate Gα subunits with a 2-fold molar excess of Gβγ. Before assay, trimers were reconstituted into phospholipid vesicles as described previously (Higashijima *et al*., 1990).

Distance Geometry Calculations. TRNOE intensities were determined by measuring the volumes of the cross-peaks and normalizing them with respect to a well-resolved diagonal peak (Met[9] Cγ protons). This process allows comparison of intensities between different experiments. TRNOE intensities were further normalized according to the number of protons involved in a given TRNOE by dividing the TRNOE intensity between resonances a and b by the normalization factor $[2N_aN_b/(N_a + N_b)]$, where N_a and N_b are the number of chemically equivalent protons under resonance a and b, respectively (Williamson & Neuhaus, 1987). These TRNOE magnitudes were then converted to distance constraints for distance geometry calculations. The TRNOEs were classified as strong, medium, or weak in intensity on the basis of the normalized intensities: 0.5−1.5%, weak; 1.5−5.0%, medium; and >5%, strong. Upper bounds for the corresponding interproton distances were 4, 3.3, and 2.7 Å, respectively. The distance between aromatic Trp[3] protons (∼2.5 Å), which is conformation-independent, together with the inverse sixth power dependence of TRNOE intensity on interproton distance were used to define these limits. Thus, for TRNOEs in these ranges, the chosen upper bounds represent conservative (loose) constraints. Methyl and methylene groups were replaced by pseudo-atoms at their corresponding centers of mass, and the upper bounds were corrected appropriately by adding 1.5 and 1 Å, respectively. Distance constraints were incorporated into distance geometry calculation in the form of skewed biharmonic potential energy functions, with a force constant of 50 kcal mol^{-1} $Å^{-2}$. Distance geometry (DG) calculations were carried out using the program DGII within Insight (NMRchitect, Biosym Technologies, San Diego, CA) on a Silicon Graphics Personal Iris workstation. The DGII program is based on the EMBED algorithm (Kuntz *et al*., 1989; Havel, 1991) and consists of the following steps. (1) The constraints used in distance geometry include covalent and chirality constraints in addition to the experimentally determined distance constraints. "Bound smoothing" is carried out to compute a complete and more precise set of bounds, given the incomplete and imprecise set of distance bounds that are experimentally available. (2) "Embedding" involves selecting a value between the lower and upper bounds obtained by bound smoothing and finding atomic coordinates that yield calculated distances which are "best-fit" to this guess. (3) In order to reduce the violations of the constraints by the embedded coordinates to an acceptable level, further optimization is carried out. This involves minimizing a function called "error function" which measures the total violation of the constraints (that include covalent and chirality constraints) by the coordinates. This minimization is done using a simulated annealing protocol followed by conjugate gradient minimization. Twenty distance geometry conformations were calculated. The structures obtained after DG calculation were further refined by restrained energy minimization using a consistent valence force field (Dauber-Osguthorpe *et al*., 1988) without Morse and cross terms. Conjugate gradient minimization was employed to yield a maximum derivative of <0.001 kcal mol^{-1} $Å^{-2}$. Charge interactions were not included during this minimization because the dielectric environment of the bound form is unknown. The structures obtained after this minimization were analyzed for their violations from the input distance constraints and convergence of backbone conformation to obtain converged, distance-based structures.

RESULTS

MP-S Preferentially activates G_s. In attempts to generate MP analogs that display a convenient dispersion of ^{1}H chemical shifts, we synthesized the peptide described here as MP-S. Screens of its activity as a regulator of nucleotide exchange on several G proteins indicated that it was relatively more effective as an activator of G_s (Figure 1), which is unusual for mastoparans, which are generally selective for the G_i family, including G_o (Higashijima *et al*., 1987, and other unpublished data). The data show that MP-S preferentially stimulated steady-state GTP hydrolysis by G_s, which contrasts with the preference of Mas7 for G_i and G_o. MP itself is also selective for G_i and G_o relative to G_s, although its maximum activity is lower (Higashijima *et al*., 1987). Neither MP-S nor Mas7 is comparably active on G_q (less than 4-fold maximum stimulation; data not shown).

Addition of Substoichiometric Amounts of G Protein Broadens the ^{1}H-NMR Spectrum of MP-S. Figure 2 shows the effect of $G_s\alpha$ on the ^{1}H-NMR spectrum of MP-S. At a protein:peptide ratio of 1:13 (2.5 mM peptide), $G_s\alpha$ caused a fairly uniform broadening of the peptide proton resonances. Small changes in chemical shifts could be detected relative

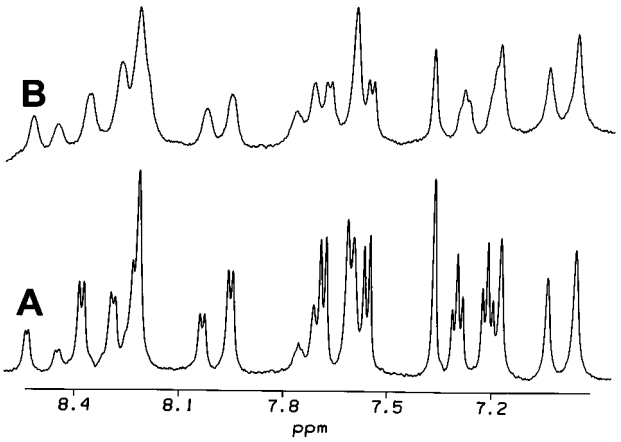

FIGURE 2: Amide region of the 500 MHz ^{1}H-NMR spectrum of MP-S in the absence (A) and in the presence (B) of r$G_s\alpha$. Spectra were recorded in 5 mM KP_i and 25 mM NaCl at pH 6.0 and 20 °C. The peptide concentration was 2.5 mM, and the protein concentration was 200 μM. No line broadening was applied prior to Fourier transformation.

to those of the free peptide. Changes were <7 Hz, both upfield and downfield. The observed broadening suggests that the free peptide is in chemical exchange with the bound form and is consistent with rapid exchange between the free and the protein-bound forms of MP-S. Exchange that is fast relative to the chemical shift time scale is expected to produce line widths and chemical shifts that are weighted averages of the free and the bound forms. The chemical shifts, therefore, are dominated by those of free peptide which is in vast molar excess.

Resonance Assignments of MP-S. Sequence-specific resonance assignments were carried out using TOCSY (data not shown) and TRNOESY (Figure 3A−C) spectra obtained in the presence of $G_s\alpha$. The presence of several unique spin systems in the sequence of MP-S made sequence-specific assignments straightforward. Trp^3, Gly^5, Ala^6, Ser^8, Aib^{10}, and Val^{13} all have unique spin connectivities and were used as starting points for assignment. Sequential TRNOEs were then used to complete assignments (Wuthrich *et al*., 1983; Wuthrich, 1986). Chemical shifts are listed in Table 1.

TRNOESY. The NOESY spectrum of MP-S alone did not show any NOEs other than weak (<0.3%) NOEs between aromatic protons and a few intraresidue NOEs corresponding to the side chains of Lys^4 and Ile^6. The absence of strong NOEs is consistent with the expectation for a small peptide like MP-S ($\omega\tau_c \sim 1$, where magnitudes of NOEs are close to zero). In contrast, the TRNOESY spectrum of MP-S in the presence of $G_s\alpha$ showed strong TRNOEs. Figure 3A−C and Figure 4A show various regions of the TRNOESY spectrum of MP-S (2.5 mM) obtained at a protein:peptide ratio of 1:19 (~5% of peptide bound). These are NOEs transferred from the bound state and reflect the conformation of MP-S bound to G protein. A similar pattern of TRNOEs was observed in the presence of $G_i\alpha$ and $G_o\alpha$, under comparable conditions (data not shown), suggesting that the conformations of MP-S when bound to these G protein α-subunits are very similar to its G_s-bound conformation.

Mastoparans bind both to detergent micelles and to phospholipid vesicles, and clear TRNOESY spectra of MP-S were also obtained in the presence of small unilamellar vesicles prepared from perdeuterated DPPC (DPPC-d_{80}) (Figure 3D−F and Figure 4B). Comparison of these spectra with those obtained in the presence of $G_s\alpha$ indicates which features of the G protein-bound conformation of MP-S are unique and, by inference, which structural features may be important for G protein regulation. TRNOESY spectra were recorded at a series of lipid concentrations. The spectra shown in Figures 3D−F and 4B, obtained at 1.6 mM DPPC-d_{80}, had the best signal-to-noise ratio. This lipid concentration is estimated to produce ~0.8% of the bound form according to titrations of MP-X with DPPC in which CD spectra were used to monitor lipid-induced change in the conformation of MP-X. These TRNOEs reflect the conformation of MP-S bound to DPPC vesicles and are not a result of viscosity changes that accompany the addition of DPPC vesicles to aqueous solution of MP-S. Addition of lipid vesicles to a final concentration of 1.6 mM increased the viscosity by only 5% at 20 °C which is expected to cause similarly small changes in the rotational correlation time and is not expected to give rise to the observed strong negative TRNOEs. Also, the observed TRNOEs which are indicative of a helical conformation are not expected from the free peptide which is predominantly random coil as shown by CD. Although the TRNOEs observed in the presence of G proteins and DPPC vesicles were similar, there were important differences which will be discussed below.

Figure 5 summarizes the sequential and medium range TRNOEs observed in the TRNOESY spectra of MP-S obtained in the presence of either $G_s\alpha$ (Figure 5A) or DPPC-d_{80}(Figure 5B). Several TRNOEs characteristic of a helical conformation were observed in both cases. For example, several sequential amide−amide TRNOEs and medium range TRNOEs between i and $i + 3$ residues were observed both in the G_s-bound form and in the lipid-bound form. Both classes of NOEs are characteristic of an α-helical conformation. However, there were important differences between the two data sets. For example, several medium range TRNOEs between Asn^2 and Gly^5 (N2 amide−G5α), Trp^3 and Ile^6 (W3Hα−I6β), Gly^5 and Ser^8 (G5α-S8N), and Ser^8- and Arg^{11} (S8α−R11β_1, S8α−R11β_2, and S8α−R11N), which would be expected from a helical structure, were absent in spectra of G_s-bound MP-S. These TRNOEs were present in spectra of lipid-bound MP-S (Figures 3B,E, and 4). The absence of these medium range TRNOEs was reproducible in experiments repeated under identical conditions and in TRNOESY spectra obtained at higher protein concentrations (protein:peptide ratios of 1:13). In addition, the TRNOEs between the side chains of Trp^3 and Ile^6 were stronger for G_s-bound MP-S than for lipid-bound MP-S.

MP-S Binds to $G_s\alpha$ as a Kinked Helix and to DPPC-d_{80} Vesicles as a Straight Helix. We used distance geometry calculations to solve the structures of $G_s\alpha$-bound and DPPC-bound MP-S based on the observed TRNOE spectra. Distance geometry calculations yield molecular conformations that satisfy NMR-derived distance constraints starting from randomized coordinates, thus avoiding the bias involved in algorithms that start from an explicit initial model. Optimized distance geometry structures were obtained starting from 20 random coordinate sets. Table 2 lists the structural statistics for MP-S bound to $G_s\alpha$ and DPPC vesicles. In the case of MP-S bound to $G_s\alpha$, the 11 structures with the lowest overall energies all had maximum violations of distance constraints of <0.2 Å and displayed similar backbone conformations from residues 3 through 12. The rmsd values for superimposing the backbone atoms of

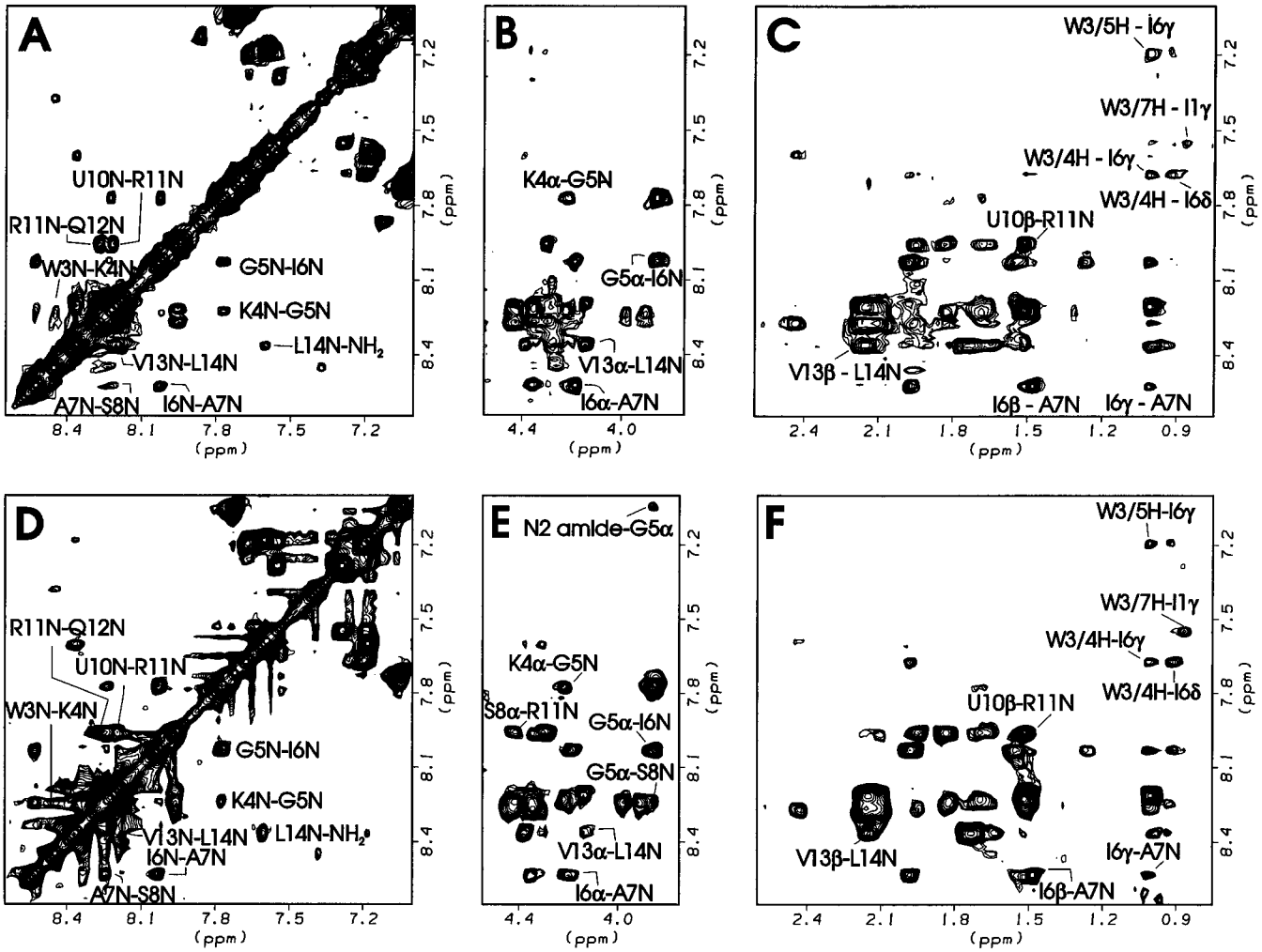

FIGURE 3: Different regions of the TRNOESY spectrum of MP-S in the presence of $rG_s\alpha$ (A−C) and small unilamellar vesicles of DPPC-d_{80} (D−F): A and D, amide−amide region; B and E, amide−α region; and C and F, amide−side chain region. Inter-residue TRNOEs are labeled. Spectra were recorded in 5 mM KP_i and 25 mM NaCl at pH 6 and 20 °C. The peptide concentration was 2.5 mM, the protein concentration 130 μM, and the lipid concentration 1.6 mM.

Table 1: ^{1}H NMR Chemical Shifts of MP-S at pH 6.0 and 20 °C

residue	NH	α	β	others
Ile[1]		3.77	1.82	γ_2, 1.43, 1.14; γ_3, 0.87; δ, 0.77
Asn[2]			2.93, 2.83	side chain amide, 7.71, 7.04
Trp[3]	8.45	4.67	3.38, 3.31	2H, 7.37; 4H, 7.68; 5H, 7.21; 6H, 7.30; 7H, 7.56; indole, 10.27
Lys[4]	8.22	4.23	1.82	γ, 1.31; δ, 1.69; ϵ, 3.01
Gly[5]	7.76	3.86		
Ile[6]	8.03	4.20	1.98	γ_2, 1.57, 1.28; γ_3, 1.02; δ, 0.93
Ala[7]	8.53	4.36	1.48	
Ser[8]	8.22	4.45	3.98, 3.91	
Met[9]	8.29	4.45	2.18, 2.08	γ, 2.67, 2.58
Aib[10]	8.22		1.52	
Arg[11]	7.95	4.32	1.96, 1.84	γ, 1.69; δ, 3.25
Gln[12]	8.29	4.35	2.17, 2.12	γ, 2.44; side chain amide, 7.60, 6.96
Val[13]	8.23	4.15	2.16, 2.13	γ, 1.01
Leu[14]	8.38	4.40	1.75	γ, 1.66; δ, 0.94, 1.00; carboxamide, 7.62, 7.18

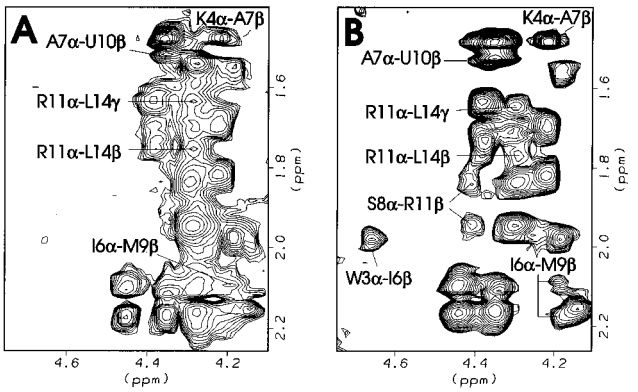

FIGURE 4: α-Side chain region of TRNOESY spectrum of MP-S in the presence of $rG_s\alpha$ (A) and small unilamellar vesicles of DPPC-d_{80} (B). Inter-residue TRNOEs are labeled. Spectra were recorded in 5 mM KP_i and 25 mM NaCl at pH 6 and 20 °C. The peptide concentration was 2.5 mM, the protein concentration 130 μM, and the lipid concentration 1.6 mM.

residues 3−12 on the average structure were 1.61 ± 0.23 Å. The backbone atoms of these structures, from residues 3 through 12, are superimposed in Figure 6A.

The structure of $G_s\alpha$-bound MP-S derived from the TRNOE data (Figure 6) is predominantly α-helical, but a consistent kink at residue 9 results in greater proximity of the N and C termini compared to those of a straight helix. The concave side of the kinked helix is hydrophobic, and polar residues are arrayed on the convex side of the molecule. The positions of the two N- and C-terminal residues are not well-defined by NOE distance constraints and may not assume a fixed position even when MP-S is bound to $G_s\alpha$.

The kinked structure of G_s-bound MP-S differs from its lipid-bound conformation. The conformation of MP-S when

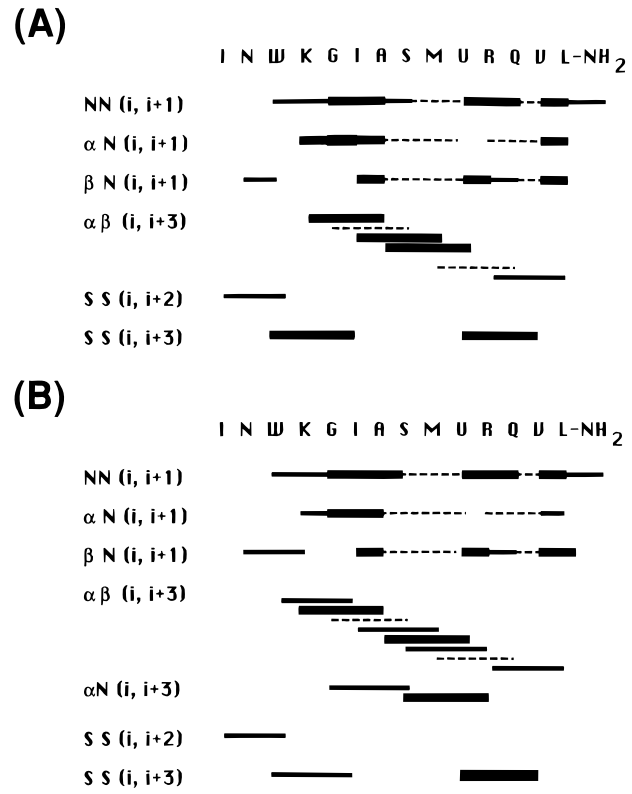

FIGURE 5: Summary of sequential and medium range TRNOEs observed in the TRNOESY spectra of MP-S in the presence of $rG_s\alpha$ (A) and DPPC-d_{80} vesicles (B). The thickness of the bar reflects the intensity of the cross-peaks. Dashed lines represent TRNOEs that might be present but that cannot be detected because of overlap of resonances. SS is used to denote TRNOEs between side chain protons. U in the sequence at the top denotes α-aminoisobutyric acid.

bound to DPPC vesicles was determined from TRNOE data using distance geometry calculations, as described above. Solutions of the DPPC-bound structures also converged well, but produced a straight helix with no obvious bend. Figure 7A shows the superposition of the best 15 of 20 DG structures, all of which had a maximum violation of <0.2 Å from the input distance constraints. The rmsd values for superimposing the backbone atoms of residues 1−14 on the average structure were 1.2 ± 0.33 Å.

The difference between the TRNOE spectra of G_s-bound and lipid-bound MP-S that accounts for the convergence on a kinked structure for G_s-bound MP-S appears to be the absence of TRNOEs between residues 8 and 11. Mock distance geometry calculations that included the distance constraints corresponding to medium range TRNOEs between residues 8 and 11 yielded helical structures devoid of a kink. The absence of medium range TRNOEs between residues 8 and 11 in G_s-bound MP-S appears to reflect the distance between these residues. The absence of these TRNOEs could conceivably result from internal motions or the presence of alternative relaxation pathways for these protons. However, these effects would be expected to affect intraresidue TRNOEs in a similar fashion, and the fact that intraresidue α → β TRNOEs of residues 8 and 11 had intensities comparable to those observed with lipid-bound MP-S suggests that the absence of medium range TRNOEs between residues 8 and 11 in G_s-bound MP-S is a result of conformational differences between the G_s-bound and DPPC-bound MP-S. Other medium range TRNOEs, K4α−A7β, I6α−M9β, A7α−U10β, and R11α−L14β, are present in both the G_s-bound and DPPC-bound MP-S. While the W3α−I6β TRNOE is close to the noise level in G_s-bound MP-S, there are other TRNOEs between the side chains of these two residues (Figure 3C) that suggest proximity of these two residues, consistent with an α-helical conformation. Thus, the striking absence of all three medium range TRNOEs between residues 8 and 11, S8α−R11β_1, S8α−

Table 2: Structural Statistics for MP-S Bound to $G_s\alpha$ and DPPC Vesicles[a]

parameter	MP-S bound to $G_s\alpha$	MP-S bound to DPPC vesicles
TRNOE-derived distance constraints		
total	130	133
intraresidue	99[b]	94
sequential	20	22
medium range	11	17[c]
residual TRNOE distance constraint violations		
number > 0.1 Å	6 ± 1.3 (4−8)	4 ± 1.5 (2−8)
total violation (Å)	1.32 ± 0.22 (1−1.74)	0.95 ± 0.35 (0.61−1.82)
maximum (Å)	0.18 ± 0.04 (0.13−0.28)	0.16 ± 0.03 (0.13−0.27)
DGII error function[d]	0.17 ± 0.07 (0.1−0.31)	0.1 ± 0.1 (0.05−0.5)
energy[e] (kcal/mol)	212.2 ± 12.5 (193−236)	204.5 ± 18.9 (188−242)
deviations from idealized geometry[f]		
bond lengths (Å)[g]	0.022 ± 0.012 (1.14 ± 0.62)	0.022 ± 0.012 (1.18 ± 0.6)
bond angles (deg)[h]	0.88 ± 2.6 (0.95 ± 0.96)	0.83 ± 2.5 (0.96 ± 0.9)
ω (deg)	8.0 ± 6.1 (1.37 ± 1.05)	9.7 ± 8.9 (1.67 ± 1.53)
Cα chirality[i]	2.9 ± 1.7 (0.83 ± 0.5)	2.9 ± 2.3 (0.83 ± 0.66)
rmsd values (Å)[j]		
backbone (1−14)	2.07 ± 0.29 (1.67−2.4)	1.2 ± 0.33 (0.82−1.96)
backbone (3−12)	1.61 ± 0.23 (1.15−1.92)	0.9 ± 0.23 (0.62−1.29)

[a] The statistics are for 20 distance geometry conformations, except for rmsd values and for deviations from idealized geometry, where the values represent 11 out of the 20 and 15 out of the 20 best conformations for $G_s\alpha$-bound and DPPC-bound MP-S, respectively. The values in parentheses represent the actual range of values, except for deviations from idealized geometry, where the values in parentheses represent the number of standard deviations from the mean reference values. [b] The additional intraresidue NOEs are exclusively from the side chain of Ile[1]. [c] The additional medium range NOEs are N2Hδ−G5Hα, W3Hα−I6Hβ, G5Hα−S8HN, S8Hα−R11HN, S8Hα−R11Hβ_1, and S8Hα−R11Hβ_2. [d] The error function measures the total violation of the constraints, which include covalent distance constraints, chirality constraints, and TRNOE-derived distance constraints, and is minimized using a simulated annealing protocol followed by conjugate gradient minimization. [e] Energy after restrained energy minimization using a CVFF force field. [f] The values in parentheses represent the number of standard deviations from the mean reference values. [g] Bond lengths include N−C, C−O, Cα−C, Cα−Cβ, and N−Cα. [h] Bond angles include C−N−Cα, Cα−C−N, Cα−C−O, Cβ−Cα−C, N−Cα−C, N−Cα−Cβ, and O−C−N. [i] Measured by the torsion angle Cα−C−N−Cβ. [j] An average of 20 distance geometry structures was used as the target for superimposition.

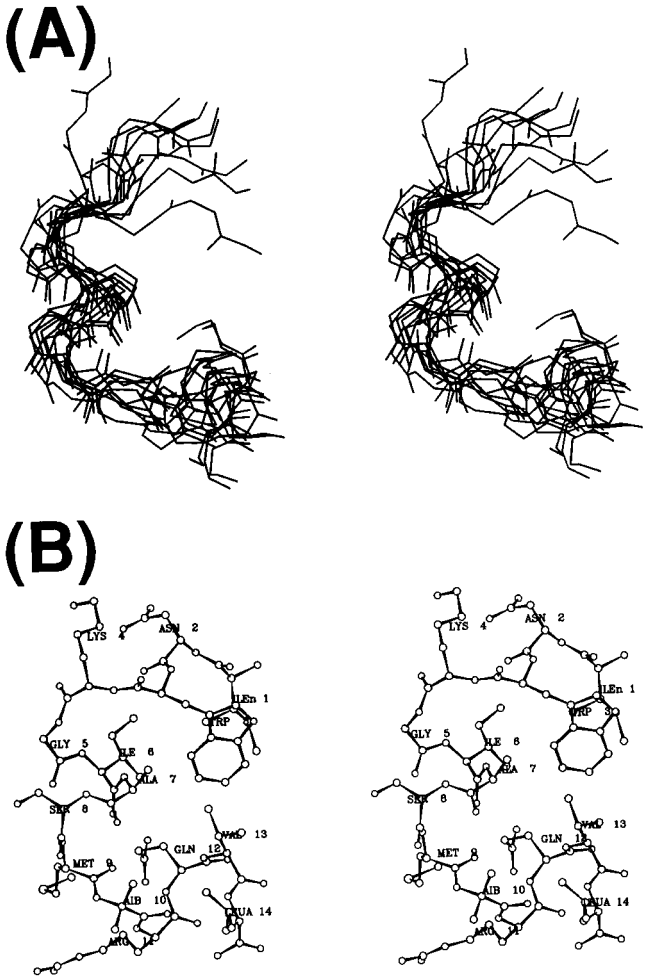

FIGURE 6: (A) Stereoview of superposition of distance geometry structures of MP-S bound to $rG_s\alpha$ calculated using TRNOE-derived distance constraints. Only the backbone atoms are shown (B) Structure with the lowest energy and least violation of the distance constraints. Only the heavy atoms are shown for clarity.

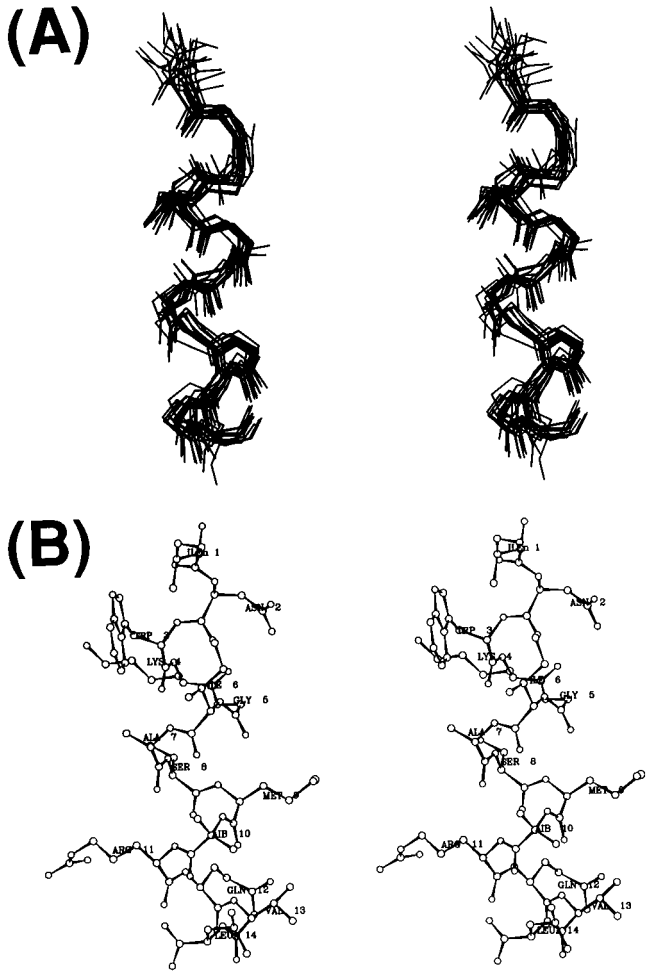

FIGURE 7: (A) Stereoview of superposition of distance geometry structures of MP-S bound to DPPC-d_{80} vesicles calculated using TRNOE-derived distance constraints. Only the backbone atoms are shown. (B) Structure with the lowest energy and least violation of the distance constraints. Only the heavy atoms are shown for clarity.

R11β_2, and S8α−R11N in G_s-bound MP-S, even in spectra recorded at higher protein concentrations (protein:peptide ratios of 1:13) is a consequence and indication of the kinked conformation of the G_s-bound MP-S.

DISCUSSION

The conformation of G_s-bound MP-S reported here is a novel one for G protein-regulating peptides in that its generally helical structure is broken by a kink around residue 9. This kink creates a more compact structure and brings the N- and C-terminal parts of the molecule closer together. The overall bend in the molecule places the hydrophobic residues on the concave side of the molecule, forming a hydrophobic pocket, and exposes the more polar, cationic side chains. Although the TRNOE data do not clearly fix the conformations of terminal residues 1, 2, 13, or 14 and these residues may be quite flexible in the G_s-bound peptide (see below), the overall structure is well-defined.

MP-S is one of a few mastoparan analogs that is an effective regulator of G_s. The TRNOE spectra of MP-S when in the presence of $G_s\alpha$, $G_o\alpha$, or $G_i\alpha$ are all very similar (data not shown), suggesting that MP-S adopts the same conformation when bound to any G protein. Specifically, the TRNOEs between residues 8 and 11 that would indicate a linear helix are absent from the spectra of MP-S bound to all three G proteins. A likely explanation for the specificity of MP-S for activating $G_s\alpha$ is that the kinked conformation is optimal for activating G_s, whereas a straight helix is the optimal conformation for activating G_i and G_o. However, correlation of the differences in the specificities of MP-X for G_i and G_o and MP-S for G_s with differences in their G protein-bound conformations is made difficult because the G_i/G_o-bound conformation of MP-X is poorly defined, with regard to a kinked versus straight helix, due to the overlap of resonances (Sukumar & Higashijima, 1992). This correlation obviously needs to be pursued.

Structure−activity studies of mastoparan analogs have shown that positive charges are crucial for regulatory activity. Thus, it is likely that at least part of the hydrophilic side of the amphipathic MP-S molecule interacts with $G_s\alpha$. If true, this orientation leaves the hydrophobic face of the peptide exposed to the environment unless it is bound to a complementary hydrophobic surface of $G_s\alpha$. The kinked structure collapses the hydrophobic face of the MP-S molecule to form a pocket that can be more easily filled by apolar residues of $G_s\alpha$. In contrast, a linear amphipathic helix of MP-S is more easily accommodated at a planar lipid−water interface, which probably explains why MP-S assumes a linear helix when bound to DPPC vesicles. Interaction of MP-S with its helix axis parallel to the surface of the bilayer would leave the hydrophobic face of the molecule buried in the hydrophobic

core of the lipid bilayer, exposing positive charges to water. Such an orientation may play a role in presenting mastoparans to G proteins.

The G protein-bound structure for MP-S is an attractive starting point for design of more selective, effective, and/or potent G_s-activating peptides. One direction for design is stabilization of the kink. Examination of the minimum energy structure in Figure 5B shows that the dihedral angles of residue 9 deviate from the helical dihedral angles of the neighboring residues and are close to those of the β-region ($\phi \sim -70°$, $\psi \sim +150°$). The kink at position 9 should therefore be stabilized by a proline residue at position 10. The right-handed helical region of conformational space is inaccessible for residues preceding proline (Schimmel & Flory, 1968), and amino acids that precede proline in natural proteins exhibit an overwhelming preference for the β-region (Macarthur & Thornton, 1991). The absence of an amide hydrogen on proline should also disrupt the intramolecular hydrogen bonding pattern of a straight helix (see below). The α-helical region is, however, entirely accessible for proline itself (Macarthur & Thornton, 1991), and a Pro^{10} analog of MP-S would thus be expected to constrain the conformation to a kinked structure. It is possible that interactions involving the Aib^{10} side chain are important for activation, and the proline ring may have to be appropriately modified if the proline analog has diminished activity.

An alternative design strategy is to destabilize a straight helix by replacing amino acids at specific positions with *N*-methyl amino acids, thus interfering with the intramolecular hydrogen bonding pattern. Preliminary modeling suggests that the kink in G_s-bound MP-S lacks hydrogen bonds involving amide groups of residues 10−12. Thus, an analog of MP-S in which these residues are replaced by the corresponding *N*-methyl amino acids is likely to have a destabilized helix. This strategy has the virtue of keeping the side chains intact while stabilizing the active conformation. Preliminary experiments that followed the dependence of specific TRNOE intensities on the mole fraction of the bound MP-S showed that the side chains of the C-terminal residues Val^{13} and Leu^{14} may not interact directly with $G_s\alpha$. The possibility that the side chains of the C-terminal amino acids might not be involved in direct interaction is useful in the design of G_s-activating peptides with reduced lytic activity. Many mastoparan analogs exhibit some lytic activity at concentrations exceeding 10 μM, which is undesirable for *in vivo* studies. However, mastoparan analogs that differ at position 10 have markedly different lytic activities (H. Mukai and T. Higashijima, unpublished), and alteration of C-terminal residues may produce active peptides with reduced lytic activity.

ACKNOWLEDGMENT

We thank Drs. Maurine Linder, Ethan Lee, and Alfred G. Gilman for providing the strains of *E. coli* expressing Gα subunits, Drs. Lila M. Gierasch and Josep Rizo for critical reading of the manuscript, and Dr. Kaori Wakamatsu for a gift of perdeuterated DPPC.

REFERENCES

Campbell, A. P., & Sykes, B. D. (1991) *J. Magn. Reson. 93*, 77−92.

Campbell, A. P., & Sykes, B. (1993) *Annu. Rev. Biophys. Biomol. Struct. 22*, 99−122.

Casey, P. J., & Gilman, A. G. (1988) *J. Biol. Chem. 263*, 2577−2580.

Clore, G. M., & Gronenborn, A. M. (1982) *J. Magn. Reson. 48*, 402−417.

Clore, G. M., & Gronenborn, A. M. (1983) *J. Magn. Reson. 53*, 423−442.

Colombo, M. I., Mayorga, L. S., Nishimoto, I., Ross, E. M., & Stahl, P. D. (1994) *J. Biol. Chem. 269*, 14919−14923.

Dauber-Osguthorpe, P., Roberts, V. A., Osguthorpe, D. J., Wolff, J., Genest, M., & Hagler, A. T. (1988) *Proteins: Struct., Funct., Genet. 4*, 31−47.

Davis, D. G., & Bax, A. (1985) *J. Am. Chem. Soc. 107*, 2820−2821.

Eker, P., Holm, P. K., van Deurs, B., & Sandvig, K. (1994) *J. Biol. Chem. 269*, 18607−18615.

Havel, T. F. (1991) *Prog. Biophys. Mol. Biol. 56*, 43−78.

Higashijima, T., Wakamatsu, K., Takemitsu, M., Fujino, M., Nakajima, T., & Miyazawa, T. (1983) *FEBS Lett. 152*, 227−230.

Higashijima, T., Wakamatsu, K., Saito, K., Fujino, M., Nakajima, T., & Miyazawa, T. (1984) *Biochim. Biophys. Acta 802*, 157−161.

Higashijima, T., Ferguson, K. M., Smigel, M. D., & Gilman, A. G. (1987) *J. Biol. Chem. 262*, 757−761.

Higashijima, T., Uzu, S., Nakajima, T., & Ross, E. M. (1988) *J. Biol. Chem. 263*, 6491−6494.

Higashijima, T., Burnier, J., & Ross, E. M. (1990) *J. Biol. Chem. 265*, 14176−14186.

Itoh, H., & Gilman, A. G. (1991) *J. Biol. Chem. 266*, 16226−16231.

Jeener, J., Meier, B. H., Bachmann, P., & Ernst, R. R. (1979) *J. Chem. Phys. 71*, 4546−4553.

Karle, I. L., & Balaram, P. (1990) *Biochemistry 29*, 6747−6756.

Kumar, A., Wagner, G., Ernst, R. R., & Wuthrich, K. (1981) *J. Am. Chem. Soc. 103*, 3654−3658.

Kuntz, I. D., Thomason, J. F., & Oshiro, C. M. (1989) *Methods Enzymol. 177*, 159−204.

Linder, M. E., & Gilman, A. G. (1991) *Methods Enzymol. 195*, 202−215.

Macarthur, M. W., & Thornton, J. M. (1991) *J. Mol. Biol. 218*, 397−412.

Macura, S., Huang, Y., Suter, D., & Ernst, R. R. (1981) *J. Magn. Reson. 43*, 259−281.

Murga, C., Ruiz-Gómez, A., García-Higuera, I., Kim, C. M., Benovic, J. L., & Mayor, F., Jr. (1996) *J. Biol. Chem. 271*, 985−994.

Northup, J. K., Smigel, M. D., & Gilman, A. G. (1982) *J. Biol. Chem. 257*, 11416−11423.

O'Dowd, B. F., Lefkowitz, R. J., & Caron, M. G. (1989) *Annu. Rev. Neurosci. 12*, 67−83.

Ross, E. M. (1989) *Neuron 3*, 141−152.

Schimmel, P. R., & Flory, P. J. (1968) *J. Mol. Biol. 34*, 105−120.

Strader, C. D., Sigal, I. S., & Dixon, R. A. (1989) *FASEB J. 3*, 1825−1832.

Sukumar, M., & Higashijima, T. (1992) *J. Biol. Chem. 267*, 21421−21424.

Taylor, S. J., Chae, H. Z., Rhee, S. G., & Exton, J. H. (1991) *Nature 350*, 516−518.

Wakamatsu, K., Higashijima, T., Fujino, M., Nakajima, T., & Miyazawa, T. (1983) *FEBS Lett. 162*, 123−126.

Wakamatsu, K., Okada, A., Miyazawa, T., Ohya, M., & Higashijima, T. (1992) *Biochemistry 31*, 5654−5660.

Williamson, M. P., & Neuhaus, D. (1987) *J. Magn. Reson. 72*, 369−375.

Wuthrich, K. (1986) *NMR of Proteins and Nucleic Acids*, John Wiley and Sons, New York.

Wuthrich, K., Billeter, M., & Braun, W. (1983) *J. Mol. Biol. 169*, 949−961.

BI962356M